ELSEVIER

Atmospheric Research 75 (2005) 183–200

ATMOSPHERIC RESEARCH

www.elsevier.com/locate/atmos

A network suitable microwave radiometer for operational monitoring of the cloudy atmosphere

Thomas Rose[a,1], Susanne Crewell[b,*], Ulrich Löhnert[b,2], Clemens Simmer[c,3]

[a]*Radiometer Physics GmbH, Meckenheim, Birkenmaarstrasse 10, 53340 Meckenheim, Germany*
[b]*Meteorological Institute, University of Munich, Theresienstr.37, 80333 München, Germany*
[c]*Meteorological Institute, University Bonn, Auf dem Hügel 20, 53121 Bonn, Germany*

Received 1 February 2004; received in revised form 28 September 2004; accepted 3 December 2004

Abstract

The implementation of an operational network of microwave radiometers is presently hampered by the cost and complexity of the available instruments. For this reason, the definition and design of a low-cost microwave radiometer suitable for automatic, high-quality observations of liquid water path (LWP) were one objective of the BALTEX cloud liquid water network: CLIWA-NET. In the course of the project, it turned out that a full profiling radiometer with 14 channels can be produced at only about 30% higher cost than a classical dual-channel IWV/LWP radiometer. The profiling capability allows simultaneous observations of LWP and the lower tropospheric (0–5 km) humidity and temperature profiles with a temporal resolution of less than 10 s and a vertical resolution from 100 m to 1 km in the planetary boundary layer depending on height and atmospheric conditions. The latter is possible due to an elevation scan capability and by the implementation of a new filter bank design. The radiometer has several additional sensors

* Corresponding author. Tel.: +49 89 2180 4210; fax: +49 89 2805508.
E-mail addresses: rose@radiometer-physics.de (T. Rose), crewell@meteo.physik.uni-muenchen.de (S. Crewell), uli@meteo.physik.uni-muenchen.de (U. Löhnert), csimmer@uni-bonn.de (C. Simmer).
[1] Tel.: +49 2225 99981 22; fax: +49 2225 99981 99.
[2] Tel.: +49 89 2180 4574; fax: +49 89 2805508.
[3] Tel.: +49 228 735181; fax: +49 228 735188.

doi:10.1016/j.atmosres.2004.12.005

(temperature, humidity, pressure, rain detector and GPS) which guarantee, together with a flexible software package, the operational performance of the system with maintenance intervals of about every 3 months. The performance of the first prototype has been verified during a 3-week campaign at Cabauw, The Netherlands.

Keywords: Remote sensing; Microwave radiometry; Radiometer technology; Boundary layer profiling

1. Introduction

The prototype of a European Cloud Observation Network (ECON) was implemented as part of CLIWA-NET (Crewell et al., 2002) by co-ordinating the use of existing, mostly operational, ground-based passive microwave radiometers. In total, 14 different radiometers – most of them self-built by the partners – were used within the CLIWA-NET measurement campaigns. The radiometers were constructed with very different specifications in terms of frequency, bandwidth, integration time, angular resolution and accuracy, e.g., in total about 50 frequencies were observed. Because of the different specifications, the generation of comparable liquid water path (LWP) products from the observed brightness temperatures (TB) proved to be a major effort. This became obvious when the results were used for the evaluation of atmospheric models (van Meijgaard and Crewell, 2005). The diversity of different microwave radiometers also reflects the fact that the implementation of an operational network of microwave radiometers is presently hampered by the cost of commercially available instruments. It was therefore a major objective of CLIWA-NET to develop a network suitable low-cost microwave radiometer for measuring LWP—the key variable within CLIWA-NET.

The liquid water path can be estimated from atmospheric emission measurements in the microwave region since at these frequencies, the cloud contribution to the signal strongly increases with frequency (Fig. 1). Therefore, standard dual-channel systems measuring at two frequencies, with one close to the 22.235-GHz water vapour line and the other in a window region at higher frequencies, can simultaneously observe LWP and the integrated water vapour (IWV) (Westwater, 1978). The channel frequencies are selected in a way that the signal at the water vapour channel frequency has a nearly constant response to water vapour with height while the second channel is in an atmospheric window between the water vapour line and the strong oxygen complex at 60 GHz. Thus, the water vapour channel can be regarded as a correction term in the LWP retrieval and vice versa. Generally, the optimum frequency for IWV retrieval along the water vapour wing depends slightly on the site statistics and the beam elevation angle (Elgered, 1993). The frequencies are mostly chosen in (still) protected frequency bands reserved for passive remote sensing. LWP accuracy depends on the frequency combination, brightness temperature measurement accuracy and observation angle, and is roughly 25 g m^{-2}; it can be improved to less than 15 g m^{-2} when an additional 90-GHz channel is used (Löhnert and Crewell, 2003; Crewell and Löhnert, 2003). By combining microwave radiometer-derived LWP and cloud radar measurements, profiles of liquid water content (LWC) can be retrieved (Frisch et al., 1998; Löhnert et al., 2001, 2004).

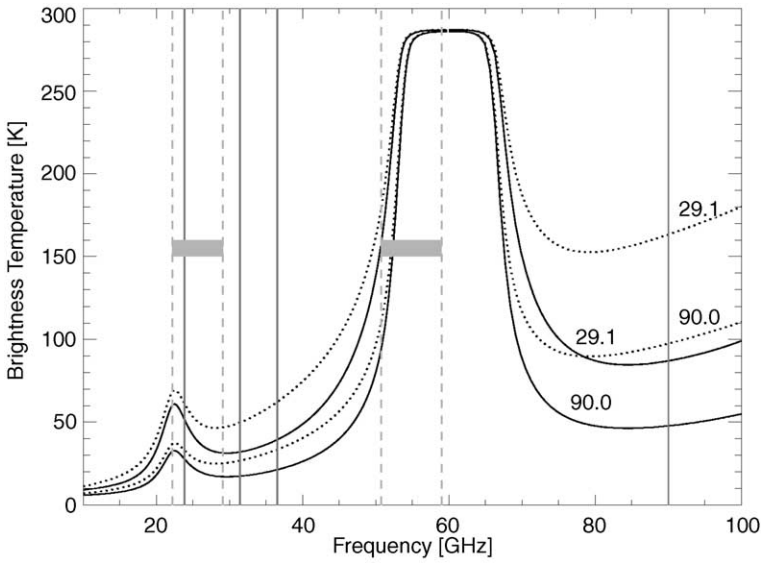

Fig. 1. Brightness temperatures at microwave frequencies simulated for clear sky (solid lines) and standard atmospheric conditions. The effect of a cloud with LWP=250 g m^{-2} is shown by the dashed lines. Values are given for zenith observations (90°) and for an elevation of 29.1°. The different possible radiometer frequencies of HATPRO are marked by vertical lines. The blocks indicate the frequency range for humidity and temperature profiling.

Profiles of water vapour and temperature can be derived from multi-spectral measurements at the wings of absorption lines or bands of water vapour and oxygen by so-called profilers, see for example (Solheim et al., 1998; Crewell et al., 2001; Ware et al., 2003). The vertical resolution of these profiles is about 1 km at 1 km height and degrades with increasing height (Güldner and Spänkuch, 2001). The vertical resolution of the temperature profile in the boundary layer can be improved by performing elevation scans at relatively opaque frequencies (Westwater et al., 1999). Since TB varies only by a few degrees at these frequencies during one scan, the radiometer needs to have very low noise. In order to optimally exploit their information content, the brightness temperatures can be combined with auxiliary information (cloud radars, lidar ceilometer, ground measurements) within the Integrated Profiling Technique (IPT) (Löhnert et al., 2004) to give simultaneous profiles of temperature, humidity and LWC. Within the design studies for the network suitable microwave radiometer cost estimates showed that a microwave profiler is only about 30% more expensive than a dual-channel system. In the following, we will focus on HATPRO (Humidity And Temperature Profiler), which has been designed as a profiling extension of the dual-channel system developed within the framework of CLIWA-NET.

The paper is organized as follows: on the basis of the experiences gained in CLIWA-NET, we first describe the requirements for a network-suited radiometer in Section 2. The microwave radiometer design that fulfills these requirements and its auxiliary components are introduced together with the control software and the retrieval process in Section 3. The performance and first atmospheric observations of a prototype instrument are

presented in Section 4. Before we conclude the paper in Section 6, we introduce the possibilities of HATPRO for boundary layer profiling.

2. Requirements and solutions

Since personnel costs contribute strongly to the total operation costs, the most important requirement for the use of any instrument within an operational network is a low-*maintenance* level. To guarantee operation control and data access even when the radiometer is situated at a remote field site, a network connection should be implemented. On the other hand, data backup within the radiometer should be possible in case of external problems. The maintenance interval is basically determined by the absolute radiometer calibration. Since absolute calibrations frequently involve the handling of liquid nitrogen, a person at the site is required. This kind of calibration is explicitly necessary for optically thick frequency channels, e.g., along the oxygen line, which cannot be calibrated using the so-called tipping curve method (Han and Westwater, 2000). To achieve maintenance intervals of several months, the radiometer needs to be extremely well thermally stabilized.

Exact timing of the measurements is necessary for almost all applications, in particular when different observations from different instruments will be combined. Therefore, synchronization of the radiometer to a standard time is necessary. If no time server can be used, GPS clocks are the preferred solution.

The radiometer must be able to operate within the range of expected *environmental conditions*. In Europe, e.g., outdoor temperatures typically range from −30 °C to +45 °C. For stable operation in this range, the inner part of the radiometer needs to be well insolated and thermally stabilized with high accuracy (±0.1 K) (see also Section 2.2). The European upper temperature threshold might be too low for tropical applications, but by increasing the lower threshold and by taking higher power consumption into account, the upper threshold can be easily shifted by 10 K. In order to resist strong winds, a robust construction of the radiometer box and a solid stand is required. The weakest structural part of the radiometer is the radome through which microwave radiation enters the receiver. Nowadays, materials transparent for microwave radiation are available which can resist harsh conditions. However, the problem of a wet radome is evident. Even with hydrophobic materials, water will still float along the radome during precipitation and influence the signal similar to rain droplets in the air. Because rain drops strongly emit and scatter microwave radiation, the signal is dominated by the drop size distribution and estimates of other atmospheric variables become difficult. Nevertheless, if radome and antenna wetting can be avoided, rain intensity and cloud water can be estimated using tilted elevation observations and polarization information (Czekala et al., 2001a,b).

2.1. Precipitation protection

The evaluation of atmospheric models (van Meijgaard and Crewell, 2005) with LWP observations turned out to be quite complex due to the contamination of the microwave radiometer measurements by precipitation either due to wetting or the precipitation signal

itself. Although many attempts (for example, see Britcliffe and Clauss (2001)) to avoid radome wetness have been made by employing strong blowers and treating the radome with hydrophobic substances, we are not aware of any working solution for zenith observations at least in moderate to strong precipitation. Therefore, it is of prime importance to detect when the onset of precipitation starts to influence the measurements. This can be detected relatively easily using close-by rain gauges or rain detectors (e.g., infrared radiometers). However, it should be noted that differences between different rain detection systems can occur due to varying time resolution, thresholds and sensitivity to wind effects. Of equal importance is to detect the time when all water is evaporated from the antenna or radome surface. Because the time required for drying depends on both instrument design and atmospheric conditions, it is nearly impossible to determine the end of the drying period of an individual radiometer without the use of simultaneous measurements by other instruments. This effect is well illustrated by simultaneous observations from four different microwave radiometers during the Microwave Intercomparison Campaign (MICAM) at Cabauw (Fig. 2).

When model forecasts are compared with the observations on a statistical basis, the filtering of precipitation events is extremely important (van Meijgaard and Crewell, 2005). But even if contaminated observations are identified, a significant amount of observation time is missing and the statistical properties of the measurements will be biased compared to a complete observation period. To solve this problem, the combination of a precipitation

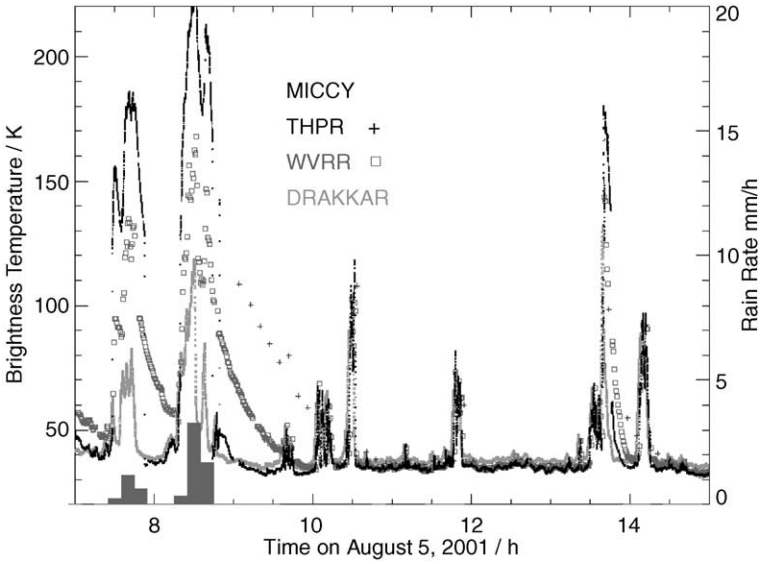

Fig. 2. Time series of 24-GHz brightness temperatures measured by four different microwave radiometers from 9 to 17 UTC on August 5, 2001 at Cabauw. In addition, rain rates observed from a close-by rain gauge are shown (grey bars). During precipitation events, the MICCY radiometer (Crewell et al., 2001) gives spurious high values due to a shutter in front of the radome. The THPR (Ware et al., 2003) and WVRR radiometers are of the same type as the ones used in the Atmospheric Radiation Measurement (ARM) program. The DRAKKAR radiometer is less affected by rain due to its small radome surface which is dried by an extremely strong blower; its small receiving area leads, however, to a large beam width of 13 deg.

detector controlling a shutter system is strongly recommended in order to reduce the periods of contaminated measurements by radome/antenna wetness. The rain detector has to be heated to remove the rain drops efficiently from the detector surface in order to determine the end of the wetting period.

When the shutter closes, the radiometer radome is protected from rain, hail and snow. A blower system can effectively dry the foil under the shutter and prevent the formation of dew or any possible condensation. If the precipitation detector indicates the end of the precipitation event, the measurements can be continued immediately. During MICAM, this approach provided the best results (see Fig. 2) and seems especially useful when precipitation occurs in the form of frequent showers.

2.2. Radiometer accuracy

The accuracy of the observed atmospheric parameters depends on the choice of frequencies and the absolute accuracy in TB. For the different microwave radiometers employed in CLIWA-NET, statistical retrieval algorithms (Löhnert and Crewell, 2003) were developed. The most suitable frequency combination for accurate LWP observations by an upward looking dual-channel system at mid-latitudes was found to be 23.8 and 36.5 GHz with an uncertainty of about 23 g m^{-2}. In these calculations, it was assumed that the absolute accuracy for TB is 1 K. While current microwave radiometers mostly have very small noise levels (<0.5 K) long-term drifts pose the more serious problem. This can only be avoided if all radiometer components are kept thermally stable. This is especially true for the optical/antenna section. As an example consider a feed horn which has a typical loss (L) of 0.6 dB (at 90 GHz). At a physical temperature of 300 K, such a feed horn contributes 45 K to the system noise. Increasing the feed horn physical temperature from 0 °C to 30 °C leads to a system noise increase of 4.5 K, which contributes to the error of the absolute brightness temperature. The situation gets more complex due to temperature gradients between the outside and the receivers. For this reason, the antenna should be thermally stabilized and insulated together with the receivers. All other critical components like the directional coupler section, the first isolator and low noise amplifiers (LNA) can be stabilized within the receiver block. Non-linearity errors of the receivers mainly caused by detector diodes should be analyzed and corrected by using a four-point calibration technique (Kazama et al., 1999) utilizing a high precision noise source injecting additional noise into the receiver input.

2.3. Temporal and spatial resolution

During MICAM, the effect of different temporal and spatial resolutions of the CLIWA-NET radiometers was investigated. It turned out that the high variability of clouds can be strongly underestimated when the integration time is too long and/or the beam width is too broad. Typically, LWP shows a correlation length of about 5 min when determined by a high resolution (1 s, 1°) radiometer. With a radiometer using the same integration time but a beam width of 13°, the apparent correlation length is 10 min. Radiometers with intermediate resolutions showed intermediate effects. To resolve cloud variability for comparison with numerical weather prediction models (NWP), a beam width of <3° and

an integration time of <20 s is recommended to achieve a resolution which is at least as good as state of the art NWP models. These resolutions should also be sufficient for the detection and evaluation of water vapour variations.

Even if LWP is not the parameter of interest, the high cloud variability determines the necessary resolution under cloud conditions since all TB include contributions by cloud liquid water. Because the measured TB are not linearly related to liquid water, geophysical parameters derived from averaged TB will be in error with increasing averaging intervals. In synthesizer-controlled receivers, the different frequency channels are measured in temporal sequence. Thus atmospheric conditions might change during the frequency scan. Therefore, the use of a filter bank design which simultaneously observes radiation at all frequencies is very advantageous. The full spectrum is acquired much faster (in one step instead of sequentially switching the channels by a synthesizer) giving a duty cycle close to 100%. This is also beneficial for all calibration procedures (see also Section 3.3). A gain calibration (relative calibration involving a black body at ambient temperature) takes only 20 s with a filter bank receiver but 140 s with a synthesizer-controlled radiometer (assuming 7 channels for each profiler). The interval between two subsequent gain calibrations depends on the receiver stability. With a precision thermal stabilisation 10 min can be achieved.

3. Design

Here we describe HATPRO, the radiometer (Fig. 3) which was designed to fulfill the requirements outlined above. To address as many user needs as possible, the radiometer has a modular design which allows the combination of different receivers. For that purpose, a wire grid is used in the optical section (Fig. 4) to decompose the microwave radiation entering the radiometer through the microwave transparent foil (radome) into two beams of vertical and horizontal polarization, respectively. Because the atmospheric radiation of interest is unpolarized (with the exception of rain events, see Czekala et al., 2001b), a flexible combination of two receivers of arbitrary frequency pairs is possible (Table 1). A receiving unit either consists of a single frequency channel (for example 23.8, 36.5 or 90 GHz) or a profiling unit (22–31.4 GHz or 51–58 GHz). If more units are desired, two radiometers can be operated together in a master/slave configuration.

In the optical section, the microwave radiation is focussed onto a corrugated feed horn which offers a wide frequency bandwidth (typically 30%), low cross polarization level and a rotationally symmetric beam. The horn should be as small as possible to reduce weight and costs. In order to generate a beam with the desired divergence, e.g., a beam width of 3° or less, a focussing element is needed. The use of a lens in front of the feed horn is not recommended since it introduces reflections at the dielectric surfaces and losses inside the dielectric. Therefore, an off-axis paraboloid mirror is used which has negligible losses and can simultaneously be used for an elevation scan.

The signals from each of the feed horn waveguide outputs are processed separately in two LNAs. The state of the art low noise amplifiers for the 20- to 30-GHz and 50- to 60-GHz frequency ranges offer superior performance compared to mixer front ends in terms of sensitivity. Furthermore, no mixer sideband filtering is required and local oscillator

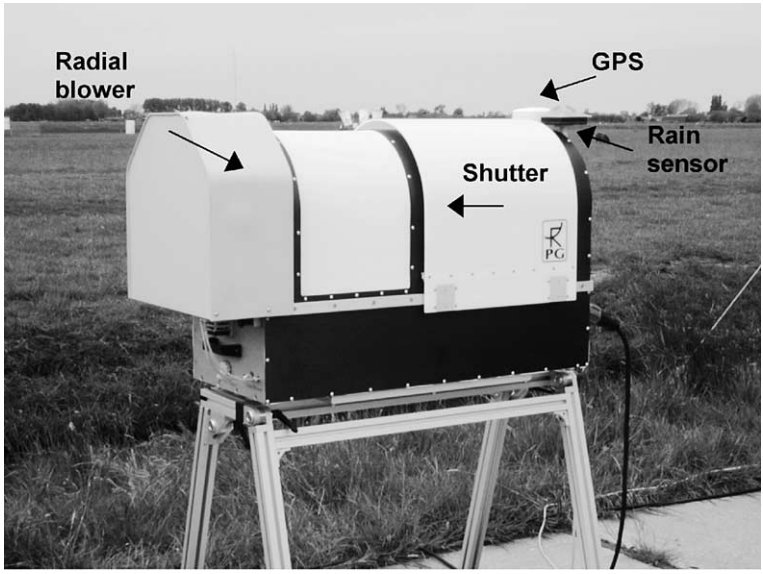

Fig. 3. Photo of the CLIWA-NET radiometer during the evaluation phase at Cabauw, The Netherlands. The radial blower has a weight of 5 kg and can easily be dismounted. This eases instrument transportation due to lower weight and better accessibility of the transportation handles.

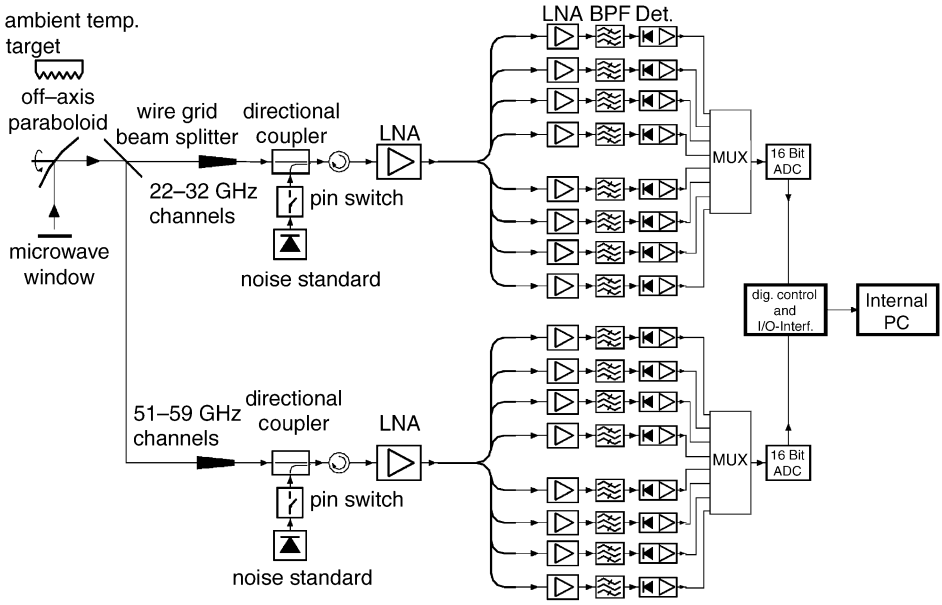

Fig. 4. Block diagram of radiometer layout for a water vapor/temperature profiler combination. The profilers can be easily replaced by single frequency channels (e.g., for LWP radiometers) by omitting the frequency splitter section.

Table 1
Possible combinations of receiving units within one radiometer

Second receiver	First receiver frequency (GHz)				
	23.8	36.5	90	22–29	50–58
–	–	–	–	LWP, q	T
23.8		LWP, IWV	LWP, IWV	–	LWP, IWV, T
36.5			LWP, IWV	LWP, q	LWP, T
90.0				LWP, q	LWP, T
22–28					LWP, q, T
50–58					

Depending on the combination, different meteorological variables can be retrieved: liquid water path (LWP), integrated water vapor (IWV), humidity (q) and temperature profile (T). IWV can be derived if the humidity profile can be retrieved. The LWP accuracy depends on the frequency combination.

frequency and amplitude drifts are avoided. Another advantage is the reduced sensitivity to interference from external signals (mobile phones, etc.) due to avoidance of frequency down conversion (no intermediate frequency generation).

For receiver calibration, a highly stabilized precision noise source can be coupled to the receiver input. This standard is calibrated during absolute system calibration (utilizing the built-in ambient temperature target and external liquid-nitrogen-cooled radiometric target). The additional noise is injected between the antenna section and the radio frequency (RF) chain, thus all RF components are calibrated (Fig. 3). The noise contribution due to antenna losses can be assumed constant as long as the physical antenna temperature is stable. The LNAs are isolated from the optical section to avoid changes of its input impedance due to antenna impedance changes caused by mirror positioning or near path obstacles. The receiver bandwidth is set by bandpass filters, which are realized in waveguide technology. The filter bandwidth for each channel is individually set to optimize the radiometric performance for lower tropospheric (0–5 km) temperature profiling (e.g., narrow bandwidth of 300 MHz for the oxygen wing frequencies at 50–54 GHz) and boundary layer profiling (e.g., wide channel bandwidth of 2 GHz for the opaque 58 GHz channel). The system gain is adjusted to deliver −30 dBm of power at the bandpass filter output which is the ideal detector input power level when an optimum linearity is required (square law regime). The detector's DC output is amplified by an ultra low drift operational amplifier chain and converted to a digital quantity by a 16-bit ADC located close to the DC-amplifier output in order to eliminate spurious noise pickup from connecting cables.

3.1. Radiometer specifications

The radiometer specifications are given in Table 2. Some highlights will be discussed in the following. For a reliable TB measurement, antenna beams must meet certain requirements. The sidelobe levels should be below −30 dB to keep TB errors below 0.2 K when the sidelobe crosses the sun. A half power beam width (HPBW) close to 3° is a compromise of spatial resolution and the design of a compact, portable instrument for field campaigns. This requirement can be achieved by a paraboloid mirror covering a projected diameter of 250 mm while illuminated by corrugated feed horns. The total weight of the radiometer is about 65 kg. In comparison, the microwave radiometer MICCY (Crewell et

Table 2
Specifications of the network suitable radiometer

Parameter	Instrument specification
System noise temperature	<800 K for 22–30 GHz profiler, 2000 K for 50.8–58.0 GHz profiler
Channel bandwidth	User selectable between 0.1 and 2 GHz
Radiometric resolution	0.2–0.4 K RMS @ 1.0 s integration time
HPBW[a]	3.5°@ 20 GHz down to 2.5°@ 90 GHz
Absolute system stability	1.0 K between 0 and 400 K
Absolute calibration	4-Point method (Kazama et al., 1999) with nonlinearity error correction, tipping curve
Internal calibration	Ambient load and precision noise standard
Temperature stabilisation	Receiver and antenna thermal stabilisation accuracy <0.1 K
Pointing speed	Elevation: 90°/s, azimuth: 10°/s (optional)
Operating temperature	−30 °C to 40 °C
Power consumption	<160 W average, 1000 W peak (incl. dew blower heater)
Input voltage	100–230 V, AC selectable, 50 to 100 Hz
Weight	<70 kg (without azimuth positioner)
Dimensions	63×40×105 cm (without azimuth positioner)

[a] Half power beam width.

al., 2001) employs a parabolic mirror with a diameter of 1 m to achieve a HPBW of 1° at all frequencies; the whole instrument weight is 2 tons.

The radiometer receivers are thermally stabilized to an accuracy of ±0.02 K which has been verified during thermo-cycles in an environmental chamber. Due to this extremely accurate stability, the receivers can run without gain calibration for almost 30 min and still maintain an absolute radiometric accuracy of ±0.3 K. This is achieved by a dual stage thermal control system consisting of a stabilized main cooler (accuracy: ±0.1 K) followed by a Peltier stage for the receivers. The thermal stabilisation was tested in an environmental chamber in the operating range of −30 °C to +45 °C. It was found that a ±0.02-K accuracy for the receiver boards can be maintained when an airflow reduction inlet is installed during winter time (T<−10 °C) which should be removed in summer. The past CLIWA-NET field experiment has supported our specified accuracy range. During measurements, the user may monitor the receiver temperatures and if desired, save them in an output file.

The radiometer is mounted on a stand about 80 cm high. The mounting plate is needed as a heat sink for the power supply unit which is thermally coupled to the bottom plate of its housing. Because exact pointing of the radiometer is required for accurate calibration (tipping curve), it needs to be accurately aligned with the horizontal plane. Therefore, we continuously monitor the inclination of the elevation axis, and the normal to the elevation axis by a two-axis inclination sensor. The reading of the sensor is used to calculate the true elevation angle. When used as a single instrument the only connections to the outside world are the main power cable (90–240 V AC, 40 to 80 Hz) and the serial interface (RS-232) cable to the external host computer.

3.2. Additional sensors and features

The radiometer includes other sensors in addition to the microwave receivers to observe environmental temperature, humidity and pressure with an accuracy of ±0.1

°C, ±1.5% relative humidity, and ±0.1 hPa, respectively. These sensors provide information about the environmental conditions and are used as input parameters for the retrieval algorithms. The barometric pressure is also used to determine the liquid nitrogen boiling temperature which is needed for absolute calibration. All meteorological sensors are accurately calibrated without the need for further recalibration. The chemically inert humidity sensor is mechanically shielded and protected by a sintered and gold plated metal dust filter. The temperature sensor is shaded and permanently exposed to a flow of air generated by a fan below the sensor cage to reduce sensor errors due to self-heating.

A specially designed precipitation sensor indicates the presence of rain or snow and controls the automatic shutter system. A GPS-Receiver provides UTC time and instrument geographical position; which provides valuable information for synchronization with satellite or other data. Since dew formation on the radome can cause TB errors of several K which are often difficult to detect during processing, a strong radial blower (Fig. 3) is implemented. Optionally an infrared radiometer can be attached externally to the radiometer housing. The serial interface connection and power supply are provided by all radiometer models to allow for later upgrades. The operating software also supports the use of an infrared radiometer for sky observations including retrieval development and simple monitoring features.

3.3. Calibration

Calibration errors are the major source of inaccuracies in radiometric measurements. The standard calibration procedure terminates the radiometer inputs successively with two absolute calibration loads which are assumed to be ideal targets, i.e., their radiometric temperatures are equal to their physical temperature. This assumption is valid with reasonable accuracy as long as proper absorber materials are chosen for the frequency bands in use and barometric pressure corrections are applied to liquid coolants when determining their boiling temperature. Another important aspect is the minimization of thermal gradients across the load which may occur for ambient loads.

The ambient load is one of the instrument's key components. The pyramidal absorber material is made from carbon loaded foam with very low thermal capacity. The load is hermetically isolated by low- and high-density Styrofoam; no exchange of air is allowed between the interior and the environment (Fig. 5). The air within the Styrofoam box is dried with silica desiccant to avoid condensation of water on the inner Styrofoam surfaces. To avoid thermal gradients across the load, it is most important that the enclosed air is subject to a closed cycle venting. The foam absorber is perforated between the pyramids such that air from the bottom of the absorber can penetrate into the volume above the pyramids. The airflow is driven by four miniature fans that maintain a steady exchange of air and thus thermal equalisation of the absorber material.

For measuring the precise temperature of the internal calibration load, the radiometer is equipped with a gauged thermo-sensor offering a guaranteed absolute accuracy of ±0.1 K. This high accuracy can only be obtained when the sensor is actively cooled to the air temperature inside the load. This is achieved by placing the sensor into the stream of air close to one of the fans. This reduces the internal thermal gradient caused by its bias

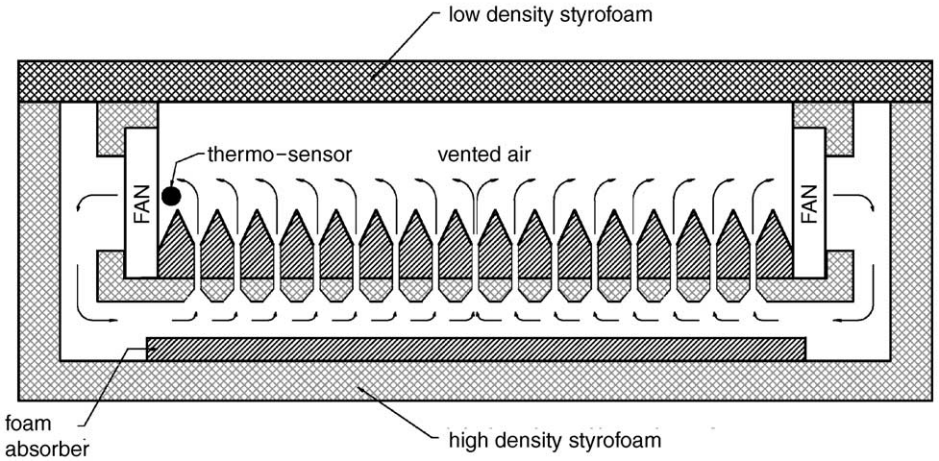

Fig. 5. Schematic illustration of ambient target (hot load). The target is not actively thermally stabilized. Instead, the black body is hermetically insulated and vented by four fans to minimize thermal gradients. A precision thermo-sensor detects the temperature of the vented air.

current. The top isolation plate is made from low-density Styrofoam with negligible microwave absorption for frequencies up to 100 GHz.

The second absolute calibration standard is a liquid-nitrogen-cooled load that is attached externally to the radiometer box during maintenance. This standard – together with the internal ambient load – is used for the absolute calibration procedure. The cooled load is stored within a 40-mm-thick polystyrene container. 13 l of liquid nitrogen (LN) is needed for one filling. The calibration error due to microwave reflections at the LN/air interface is automatically corrected by the calibration software. It is assumed that the LN surface is flat. The refractive index of LN is 1.2 at microwave frequencies which leads to a correction of +1.8 K for the target's radiometric temperature. The reflected fraction is terminated with the receiver radiometric temperature of close to 300 K (isolator termination of receiver input, see Fig. 4).

It is not convenient to use a LN-cooled load for each calibration. For this reason, the radiometer has two built-in noise sources (one for each receiver) that can be switched to the receiver inputs. The equivalent noise temperature of the diode is determined by the radiometer itself after a calibration with the two absolute standards. Its radiometric temperature should be in the order of 200 K to be comparable with the temperature difference of a LN-cooled and ambient temperature calibration standard. The noise diode is also used to correct for detector diode nonlinearity errors. The accuracy of an absolute calibration carried out with this secondary standard (replacing a LN-cooled target) and the ambient temperature load is comparable to the results obtained with a liquid-nitrogen-cooled load. The advantage of the secondary standard is obvious: a calibration can be automatically done at any time. All system parameters are recalibrated including system noise temperatures.

In addition, a tipping curve calibration (see Han and Westwater, 2000 for a detailed description) is implemented for channels with low atmospheric opacity. The atmospheric opacity is observed as a function of elevation angle θ, e.g., of air mass ($1/\sin(\theta)$). Because

an extrapolation to zero air mass should give the value for the cosmic background radiation, the receiver gain can be derived by fitting a linear function to this data set. The reliability of sky tipping calibrations strongly depends on how good the assumption of a homogeneously stratified atmosphere is. This assumption is in general violated under cloudy conditions. If desired, the user can specify time intervals for an automatic tipping curve calibration. To diagnose suitable conditions, the user can activate several in-built software checks. The most important criterion is a high linear correlation between air mass and observed opacity, which, depending on the horizontal stratification of the atmosphere, will determine if the calibration will be accepted or rejected. Experience has shown that a linear correlation of 0.999 should be reached in order to obtain an acceptable solution. Other tests the user may activate include thresholds for TB zenith observations and the corresponding variability, which may also be used to detect the unwanted presence of clouds during calibration.

3.4. Software

For operational measurements, the radiometer needs to be independent from human maintenance and has to perform many automatic tasks. This includes, e.g., the data acquisition of all housekeeping channels and detector signals, controlling of elevation stepper and shutter system, backup storage of measurement data, automatic and absolute calibration procedures, retrieval calculations, and interfacing with a potential external host. In addition, the system has to manage the Master/Slave interfacing between two instruments, when required. These tasks are handled by a built-in embedded Personal Computer (PC) with 250-MB disk on module (DOM) for data storage. The PC is designed for operating temperatures from −30 °C to 60 °C. The software running on this PC can easily be updated by a password-protected file transfer procedure between host and embedded PC. A newly developed software runs on the host PC for all Windows platforms (Windows 95, Windows 98, Windows NT4.0, Windows 2000, Windows XP). A LINUX version is under preparation. A serial interface (RS-232) is used to link host and embedded PC. Measurement Definition Files (MDF) can be set up in order to allow for radiometer measurements without connection to the controlling computer. On the other hand, the controlling computer can be connected to the Internet and data can be transferred automatically to the outside world for online use. When two radiometers are operated simultaneously, the Master is always the instrument directly connected to a host computer. On the Slave side, the host interface is left disconnected. The communication line between Master and Slave is a bi-directional symmetric parallel interface.

3.5. Retrieval algorithms

The radiometer has built-in retrievals which allow immediate graphical display of atmospheric quantities on the host computer. For that purpose, statistical algorithms are used which only use the radiometer measurements (TB, environmental temperature, pressure, humidity, IR temperature if applicable). The atmospheric parameters which can be retrieved depend on the receiver combination (Table 1). When IWV can be retrieved, the microwave wet delay is an additional output parameter.

The retrieval algorithms are developed for certain geographic regions using radiative transfer calculations performed on the basis of long-term radiosonde data sets. Multiple regression (Löhnert and Crewell, 2003) and Artificial Neural Network (ANN) algorithms are available. It should be noted that a limitation to all statistical algorithms including ANN is that they can only be applied to the range of atmospheric conditions, which are included in their training data set. Even in large training data sets, certain atmospheric condition might not be represented adequately due to the high variability of nature, the limitation of radiosonde data to fixed times, limited vertical resolution and insufficient methods to model realistic liquid water profiles from the radiosonde measurements. When extrapolations beyond the covered range of atmospheric states are made, especially ANN algorithms are prone to behave in an uncontrolled way, while simple linear regressions might still give reasonable, although erroneous, results. Linear regression methods including quadratic terms of some input variables (mostly TBs) offer the robustness of simple linear regression retrievals with the advantage to model nonlinearities much better. In regions or during seasons with likely occurrence of extreme atmospheric conditions, linear regression methods with quadratic terms are superior to ANN methods. Assuming the host computer is connected to further instruments, it is possible to run other synergetic algorithm in near online mode; however, since all measurements are stored to disk, post-processing is also possible.

4. Performance

The first prototype radiometer incorporating a humidity and a temperature profiler (HATPRO) was evaluated during the BALTEX Bridge Campaign in May 2003 at Cabauw, The Netherlands. Continuous zenith observations were performed. Here, we want to illustrate the quality of the derived IWV, LWP, temperature and humidity profiles.

Temperature and humidity profiles were retrieved using both a statistical multiple linear regression approach (see previous chapter) and the integrated profiling technique (IPT). The latter method exploits in addition to HATPRO measurements observations by a lidar ceilometer, a cloud radar, and the closest operational radiosonde ascent together with statistics from a cloud model (Löhnert et al., 2004). Both results are compared with simultaneous radiosondes. Fig. 6 shows that in two very different atmospheric conditions HATPRO is capable of retrieving accurate temperature and humidity profiles using a simple regression approach. However, sharp inversions or cloudy situations are better captured when measurements of different instruments are combined in a statistically and physically consistent way, as achieved with the IPT. It is important to note that microwave profilers such as HATPRO also lead to improved IWV and LWP estimates compared to dual-channel instruments. Crewell and Löhnert (2003) have shown that LWP and IWV errors can be reduced by 18% and 36%, respectively.

5. Boundary layer temperature profile

In order to achieve a high vertical resolution of the temperature profile in the boundary layer, elevation-scanning microwave observations can be used (Westwater et al., 1999) for

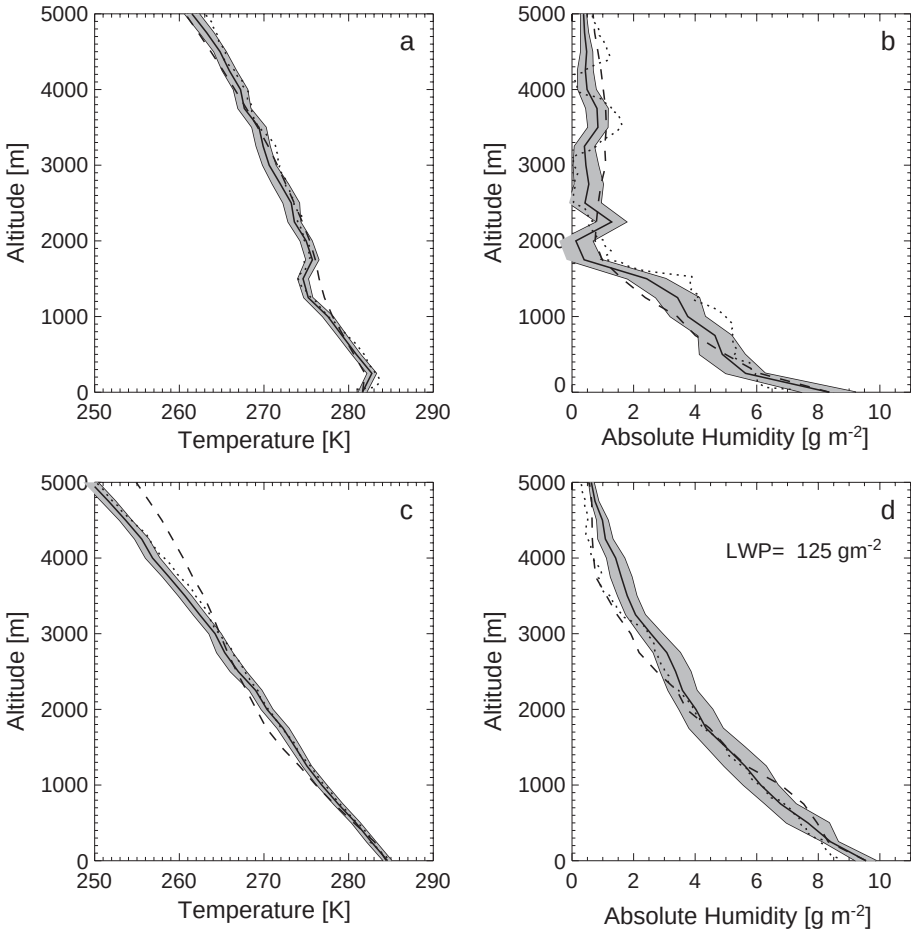

Fig. 6. Temperature and humidity profiles derived from HATPRO observations; solid lines—IPT and corresponding errors (shaded grey), dashed lines—multiple linear regression retrieval. The dotted lines denote the radiosondes. Two cases are shown: panels (a) and (b) show measurements from May 7, 6 UTC (clear-sky); panels (c) and (d) show measurements from May 20, 21 UTC (cloudy sky). Additionally, information about the retrieved LWP is given.

altitudes at least up to 1 km. For this purpose, single-channel receivers with frequencies close to the center of the oxygen complex (around 60 GHz) are employed. Assuming a stratified atmosphere, the brightness temperature observed at 0° elevation corresponds to the environmental temperature. At higher elevation angles, the fraction of radiation originating from higher atmospheric layers increases. Therefore, a monotonic decrease of atmospheric temperature with height (as for standard atmospheric conditions) leads to a monotonic TB decrease with increasing elevation angle (Fig. 1). However, temperature inversions are frequently observed. These conditions are important to detect because they inhibit vertical transport and trap pollutants close to the ground. The strong inversion case shown in Fig. 7a and c leads to a TB increase with increasing elevation angle up to 50° due

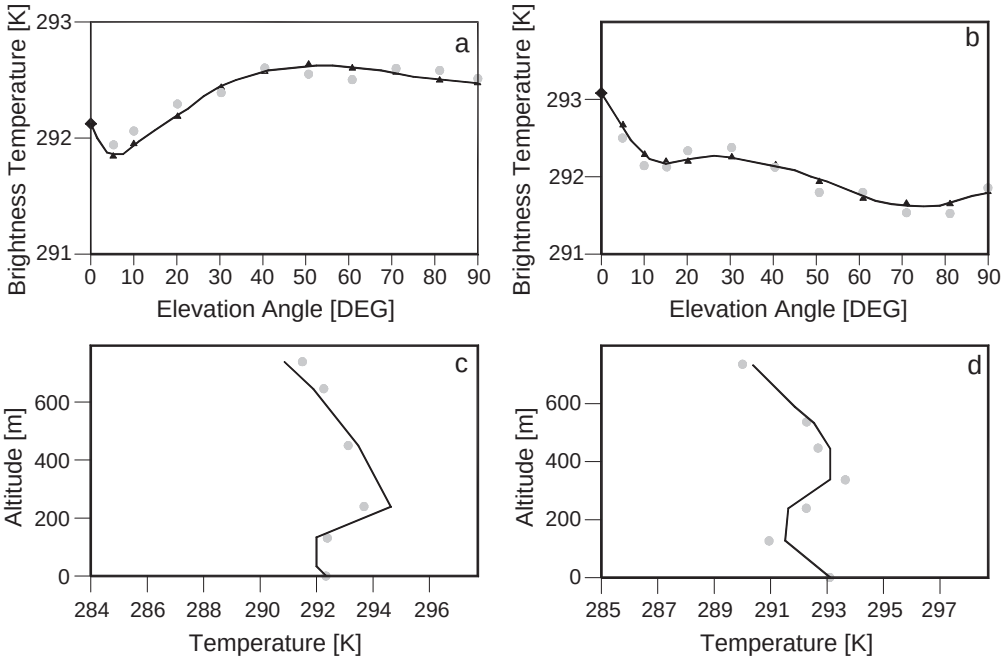

Fig. 7. Brightness temperatures at 58 GHz as a function of elevation angle for two occasions (a and b) observed with a 2 GHz (solid line) and 0.3-GHz (grey dots) bandwidth receiver. The temperature at 0° elevation was determined by using the environmental temperature sensor (black diamonds). The corresponding temperature profile retrievals (c and d) is again given for both receiver bandwidths.

to the cooler layers close to the ground. The second case exhibits a temperature profile with a more complex structure (Fig. 7d). Due to the temperature decrease with height in the lowest 150-m TB also decreases rapidly from 0 to 15° elevation. A wave-like TB structure results from the isothermal and inversion regions above.

Typical atmospheric temperature profiles cause TB variations in the range of only 1 or 2 K at 58 GHz over a complete elevation scan (Fig. 7). Extremely high receiver sensitivity is thus required to resolve the temperature profile. Commercial boundary layer profilers achieve this sensitivity by employing receivers with a wide channel bandwidth of >2 GHz. In comparison, standard microwave profilers use bandwidths of 200 to 400 MHz to accurately resolve the oxygen line shape. Accordingly, their radiometric resolution is lower by a factor of 3 compared to single channel boundary layer profilers. Due to the additional noise, artificial temperature inversions might be retrieved (see grey dots in Fig. 7c) and inversions occurring in reality might strongly smoothed (see grey dots in Fig. 7d). The impact of bandwidth for different frequencies on the temperature retrieval is nicely illustrated in Cadeddu et al. (2002). The new filter bank design in HATPRO allows for different spectral bandwidths for different frequencies; the radiometer has narrow bandwidth channels along the wing of the oxygen absorption band (where high spectral resolution is required) and a broadband (2-GHz bandwidth) channel at 58 GHz in the band center to optimize both the lower tropospheric and boundary layer profiling with one radiometer.

6. Summary and outlook

We presented HATPRO, a network suitable low-cost and low-maintenance microwave radiometer for operational monitoring of the cloudy atmosphere, which surpasses the wide range of radiometers deployed during the CLIWA-NET campaigns in several important aspects. Features like rain detection and protection, time and pointing accuracy, accurate temperature stabilization, and a fully automated software were implemented that will be beneficial for climate monitoring, data assimilation, and atmospheric model evaluation. The cost of a full profiling system with estimates of the temperature and humidity profile, which also leads to improved LWP (and IWV) estimates turned out to be only 30% higher than for a dual-channel system. The variable bandwidth for the temperature profiling channels allows for increased spatial resolution in the boundary layer using elevation scans. Adding measurements of a wind profiler, a cloud radar and/or a lidar further improvement of the quality of the derived atmospheric state parameters, can be obtained and reasonable estimates of the vertical cloud water profiles are possible.

Acknowledgements

We gratefully acknowledge the work of all MICAM participants, i.e., Lorenz Martin and Christian Mätzler (University of Bern), Gunnar Elgered (Chalmers University), Cecille Mallet and Laurent Chardenal (CETP), Jürgen Güldner (DWD) and Boris Kutuza (IRE). We would also like to thank Erik van Meijgaard (KNMI) and Harald Czekala

(RPG) for the constructive discussions. Part of this work was performed within the CLIWA-NET project sponsored by the EU under contract number EVK2CT-1999-00007.

References

Britcliffe, M.J., Clauss, R.C., 2001. The effects of water on the noise–temperature contribution of deep space network microwave feed components, TMO Progress Report 42-145, available at http://tmo.jpl.nasa.gov/tmo/progress_report/42-145/145G.pdf.

Cadeddu, M.P., Peckham, G.E., Gaffard, C., 2002. The vertical resolution of ground-based microwave radiometers analyzed through a multiresolution wavelet technique. IEEE Trans. Geosci. Remote Sens. 40 (3), 531–540.

Crewell, S., Löhnert, U., 2003. Accuracy of cloud liquid water path from ground-based microwave radiometry: Part II. Sensor accuracy and synergy. Radio Sci. 38 (3), 8042.

Crewell, S., Czekala, H., Löhnert, U., Simmer, C., Rose, T., Zimmermann, R., Zimmermann, R., 2001. MICCY—a 22 channel ground-based microwave radiometer for atmospheric research. Radio Sci. 36, 621–638.

Crewell, S., Drusch, M., Van Meijgaard, E., Van Lammeren, A., 2002. Cloud observations and modelling within the European BALTEX cloud liquid water network. Boreal Environ. Res. 7, 235–245.

Czekala, H., Crewell, S., Simmer, C., Thiele, A., 2001a. Discrimination of cloud and rain liquid water path by groundbased polarized microwave radiometry. Geophys. Res. Lett. 28, 267–270.

Czekala, H., Crewell, S., Simmer, C., Thiele, A., Hornbostel, A., Schroth, A., 2001b. Interpretation of polarization features in ground based microwave observations as caused by horizontally aligned oblate rain drops. J. Appl. Meteorol. 40, 1918–1932.

Elgered, G., 1993. Tropospheric radio-path delay from ground-based microwave radiometry. In: Janssen, M.A. (Ed.), Atmospheric Remote Sensing by Microwave Radiometry. John Wiley, New York, pp. 240–257.

Frisch, A.S., Feingold, G., Fairall, C.W., Uttal, T., Snider, J.B., 1998. On cloud radar and microwave measurements of stratus cloud liquid water profiles. J. Geophys. Res. 103, 23195–23197.

Güldner, J., Spänkuch, D., 2001. Remote sensing of the thermodynamic state of the atmospheric boundary layer by ground-based microwave radiometry. J. Atmos. Ocean. Technol. 18, 925–933.

Han, Y., Westwater, E., 2000. Analysis and improvement of tipping calibration for ground-based microwave radiometers. IEEE Trans. Geosci. Remote Sens. 38, 1260–1276.

Kazama, S., Rose, T., Zimmermann, R., Zimmermann, R., 1999. A precision autocalibrating 7 channel radiometer for environmental research applications. Jpn. J. Remote Sens. 19, 37–45.

Löhnert, U., Crewell, S., 2003. Accuracy of cloud liquid water path from ground-based microwave radiometry: Part I. Dependency on cloud model statistics and precipitation. Radio Sci. 38 (3), 8041.

Löhnert, U., Crewell, S., Macke, A., Simmer, C., 2001. Profiling cloud liquid water by combining active and passive microwave measurements with cloud model statistics. J. Atmos. Ocean. Technol. 18, 1354–1366.

Löhnert, U., Crewell, S., Simmer, C., 2004. An integrated approach towards retrieving physically consistent profiles of temperature, humidity and cloud liquid water. J. Appl. Meteorol. 43, 1295–1307.

Solheim, F., Godwin, J., Westwater, E.R., Han, Y., Keihm, S., Marsh, K., Ware, R., 1998. Radiometric profiling of temperature, water vapor and cloud liquid water using various inversion methods. Radio Sci. 33, 393–404.

van Meijgaard, E., Crewell, S., 2005. Comparison of model predicted liquid water path with ground-based measurements during CLIWA-NET. Atmos. Res. 75, 201–226.

Ware, R., Solheim, F., Carpenter, R., Gueldner, J., Liljegren, J., Nehrkorn, T., Vandenberghe, F., 2003. A multi-channel radiometric profiler of temperature, humidity and cloud liquid. Radio Sci., 38(4), 8079, 1–13.

Westwater, E., 1978. The accuracy of water vapor and cloud liquid determination by dual-frequency ground-based microwave radiometry. Radio Sci. 13, 667–685.

Westwater, E.R., Han, Y., Irisov, V.G., Leuskiy, V., Kadygrov, E.N., Viazankin, S.A., 1999. Remote sensing of boundary-layer temperature profiles by a scanning 5-mm microwave radiometer and RASS: comparison experiment. J. Atmos. Ocean. Technol. 16, 805–818.